

EVENT RECOGNITION FOR REALISTIC LOAD SPECTRA AND THEIR IMPACT ON INSPECTION INTERVALS IN DAMAGE-TOLERANT DESIGN

F. Runge*, S. Starke†, L. Markgraf‡, M. Bartelt*, P. Horst*, S. Heimbs*

* Technische Universität Braunschweig, Institute of Aircraft Design and Lightweight Structures,
Hermann-Blenk-Str. 35, 38108 Braunschweig, Germany

† IBK Innovation GmbH & Co. KG, Butendeichsweg 2, 21129 Hamburg, Germany

‡ Airbus Operations, 21129 Hamburg, Germany

Abstract

The damage tolerance behaviour for two fuselage locations is investigated. Parametric studies are performed, revealing the influence of geometry onto the inspection intervals. For a circumferential crack in the upper fuselage, the influence of multiple different flights onto the inspection intervals is investigated. Results may be used both, in preliminary aircraft design as well as structural optimisation.

Keywords

aircraft design, damage tolerance, event recognition

1. INTRODUCTION

One key role in fulfilling the demand for economic passenger aircraft is the accurate modelling of the aircraft during the preliminary design phase. In order to obtain optimal aircraft configurations the multidisciplinary character of the aircraft has to be captured within the model. Damage tolerance issues are often neglected here, because of the high computational effort it entails in order to obtain reliable results. This is mainly due to the fact that damage tolerance behaviour for metallic components is not only depending on the stress amplitudes but also on the stress history. Therefore, realistic load time histories are required.

In this paper, in-service data of a passenger aircraft is processed by an event recognition model to determine flights of different severities. Subsequently, a state-of-the-art load calculation is applied to the classified in-service data to investigate the impact of the load spectra on the inspection intervals due to damage tolerance requirements.

Therefore, a machine learning model has been developed for fast segment and event recognition of the aforementioned in-service data, i.e. an automated labelling of full flights with respect to segments like “rotation”, “climb” and “cruise” and events that occur during these segments like “lateral manoeuvre” for instance. In an ongoing task the recognition will be extended by vertical gust events including the gust severity. For this training step the “ground truth” of the gust angle must be available and is estimated using an extension of a “flight path reconstruction”. The extension of the event recognition by gusts allows it to select flights from a

larger set of in-service data with the idea to retrieve smooth flights and a flight with a high level of gust occurrences / intensities. These selected flights are processed in a digital twin model, which augments the in-service data by load-time histories for the subsequent damage tolerance analysis.

The damage tolerance behaviour is investigated for two locations of a metallic aircraft, typically driven by damage tolerance requirements, namely the upper fuselage panel and a fuselage side panel. The developed damage tolerance model features stiffened structures to be able to represent the beneficial effects of stiffeners during crack growth and uses the PREFFAS [1], [2] model to consider the load interaction effects, which is a good compromise between accuracy and low calculation effort for the parametric studies investigated here. These studies include parameters relevant for aircraft design, e.g. but not limited to: Stiffener pitch, stiffener area and skin thickness. Furthermore, the prior event recognition allows investigating the role of the flight severity on the lifetime of an aircraft (focusing on gusts)

2. STRESS TIME HISTORIES

The damage tolerance analyses are performed for ground-air-ground (GAG) cycles. The used GAG cycles within these studies are calculated from in-service data recordings of a commercial civil aircraft. The influence of up to 9 different GAG cycles is investigated here for two scenarios: A circumferential crack in the upper fuselage (scenario F) (in front of wing the connection) and an axial crack in the fuselage side panel (scenario F2).

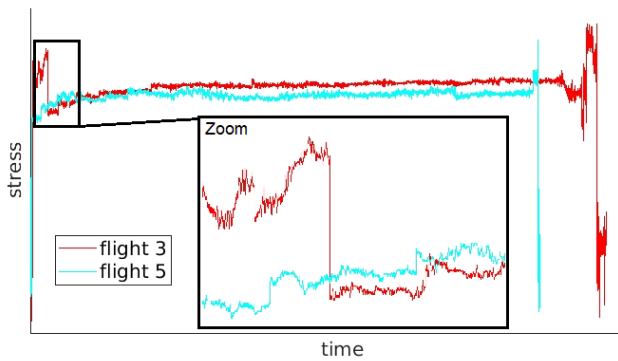


FIG 1. Normalised stress history for mid fuselage station for 2 selected flights

The qualitative stress history for scenario F is shown in Fig 1.

The GAG cycles feature ground as well as flight loads.

3. EVENT RECOGNITION MODEL

For the crack propagation analysis load time histories are required for a set of full flights covering the whole ground-air-ground cycle. Loads are estimated using an observer model which is optimised for high accuracy over all levels of intensities as required for fatigue loads assessments. In order to select interesting in-service recordings for this assessment from a larger data lake the occurrences and intensities of gust events are investigated. This step requires to extend a flight phase recognition as addressed in [3] and based on in-service recordings. For the supervised learning of a machine learning model the “ground truth” must be known which corresponds to slices from the full flight recording labelled as gusty. This could be done manually for other events like lateral manoeuvres by simply looking at corresponding signals (like the roll angle), but it is not straight forward for gusts. The vertical load factor is commonly used for this task but this signal is noisy and peaks can also correlate to manoeuvres which is addressed in [4] and [5]. For this study a Flight Path Gust Reconstruction is applied on the in-service recordings, which outputs the estimated gust angle. This estimate is used to label gusty events in the flight recordings. These “slicing tables” are applied together with the in-service recordings to train a machine learning model with an architecture based on the one described in [6] and with the main idea to cover the temporal and spatial dependencies of the signals. After training of this model on one dataset it is applied on the use-case dataset (different type of aircraft) in order to provide a “slicing table” for all flights available in the data lake. For a set of selected flights the required load time histories are computed and further processed for the assessment on crack propagation.

3.1. FPGR

FPGR („Flight Path and Gust Reconstruction“) is an extension of the “Flight Path Reconstruction” which for instance is used in scope of data preparation of flight test

data. Its method is based purely on measured data and the equation of motion. FPGR additionally allows to compute an approximation of the gust velocity, which is needed for the development of the segment and event detection of gusts. The approximation of loads is based on a model based observer. Since the processing of a complete flight is very time consuming, the computation of loads should be conducted for a selection of flights based on the results of the segment and event recognition. The vertical load factor is driven by vertical – and lateral manoeuvres as well as gusts. Its separation into counterparts for the different kind of events is discussed in [4] and [5]. Here the vertical load factor is split into two counterparts, one describing the slow motion of manoeuvres and the other one describing the fast motion of (vertical) gusts. A low pass filter with the half short period frequency as the cut of frequency is applied to create these two signals from the unbiased vertical load factor. Additionally, a dead band of 0.05g is applied as suggested by FAA for gust recognition.

3.2. Data imbalance

Most time of a standard flight is spent in a cruise condition and so some techniques are applied in order to address the resulting data imbalance when creating a training- and validation dataset as well as its impact during the training. For creation of a machine learning dataset a selection of samples is picked from a defined set of flights. For each flight the listed labels in the corresponding slicing table are used to ensure that not more than a set number of events is selected. This approach does not solve the problem of having only a single rotation and touch down segment per flight but it significantly reduces the number of more or less identical cruise events.

3.3. Assessment of flights

The selection of flights for computation of crack propagation is based on single events. For crack propagation the spectrum of the stresses of the complete flight are more relevant than single events. To include the information of the complete stress time history, delta stress values are determined between local maxima and minima of the stress history for all available flights to generate these spectra. Fig 2 shows delta stress spectra for the wing root for the average spectra of all flights available as well as for selected flights representing a flight with a low (flight 5) and a high stress (flight 3) intensity.

Tab. 1 summarises the assessment of all flights with different normalised criteria. “max. stress” is based on the highest stress value occurring during the flight and is normalised with the maximum stress of all flights. The criteria “flight duration” is based on the duration of the complete flight from start to end and normalised with the longest flight. The criteria “integral spectra” is based on the integral of the occurred delta stress values versus the occurrences per flight.

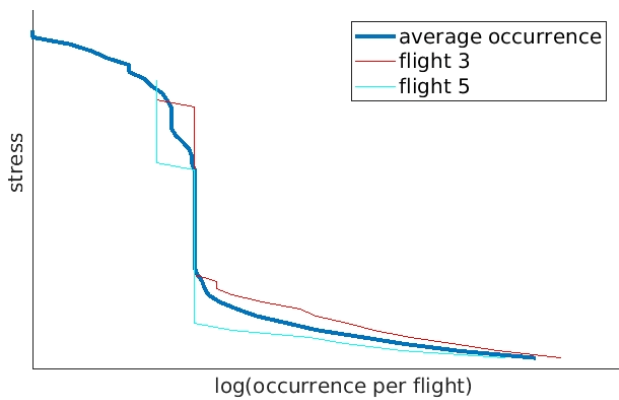


FIG 2. Occurrence of normalised delta stresses for 2 selected flights

TAB 1. Flight assessment values for scenario F

flight	max. stress	flight duration	int. spectra
1	0.9652	0.3845	0.5441
2	0.9898	0.3532	0.6537
3	0.9227	0.9621	1.0000
4	0.9861	1.0000	0.9933
5	0.8488	0.8524	0.6541
6	0.9577	0.9432	0.8196
7	0.9074	0.7541	0.5744
8	0.9967	0.9159	0.9586
9	0.9636	0.4698	0.6053

4. DAMAGE TOLERANCE MODEL

Crack growth is calculated based on cycle-by-cycle SIF evaluations to capture load interaction effects, where the SIF is defined as

$$(1) \quad K = \sigma \beta \sqrt{\pi a}.$$

with the applied remote stress σ , the half crack length a and a correction factor β to account for the stiffened panel, see Sec. 4.1. The SIF is only valid within the limits of linear elastic fracture mechanics, i.e., small scale yielding. Using an empirical crack growth law, such as the well known Paris law,

$$(2) \quad \frac{da}{dN} = C \Delta K^m$$

the crack growth increment may be calculated while requiring minimal material constants C and m obtained from constant amplitude testing. Only single cracked cases are considered here. The crack is assumed to be exposed to mode 1 loading.

4.1. Stiffened panel modelling

In the following, conventional stiffener layouts are considered, i.e. that the stringers are orientated orthogonally to the frames. For scenario F, the stiffeners correspond

to stringers. For scenario F2, the stiffeners correspond to frames.

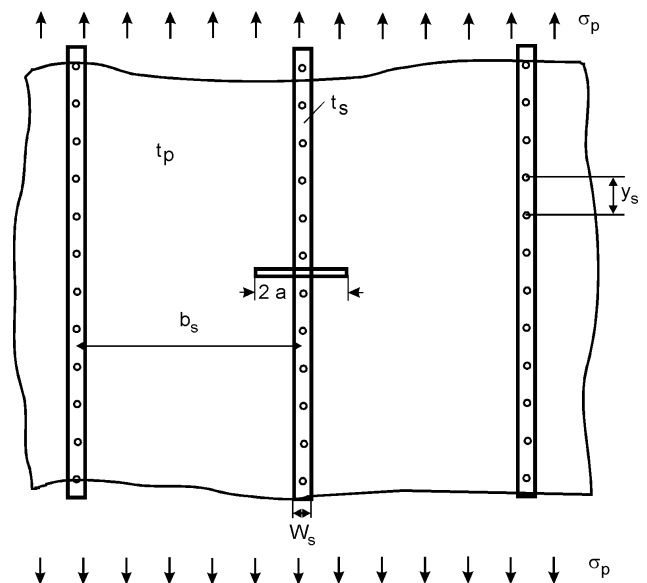


FIG 3. Stiffened panel modelling parameters (σ_p remote stress in the plate, t_p plate thickness, t_s stiffener thickness, W_s stiffener width, b_s stiffener pitch, a half crack length, y_s rivet pitch); Stringer and plate with Young's modulus E_s and E_p , respectively [7]

In [7] a chordwise crack in the lower wing panel has also been investigated.

The SIFs for the stiffened panel are calculated via a semi-analytical model based on [8], see [7] for details. The strength of the stiffeners which act to close the crack (for intact stiffeners) is governed by the axial stiffness EA_s , where E is the elastic modulus and A_s the cross-section of the stiffener. Bending stiffness contributions are not considered here, because the eccentricity of the stringers are negligible. For reasons of brevity, the stiffeners are either assumed to be intact or completely broken, although this is not a limitation of the model. In fact, the model allows for continuously cracking stiffeners as well. The stress in the stiffeners is checked against the yield limit. Once the yield limit is exceeded, the stiffener is set to be broken. Otherwise the stiffeners would extend the fatigue life unrealistically.

4.2. Load interaction effects

The crack closure model PREFFAS is used to model the retardation and acceleration effects during fatigue life time for plasticity induced closure. PREFFAS calculates a continuously varying opening stress value σ_{op} through out the stress spectrum. Crack closure models assume that only the stress range where the crack is open (when the stress is above σ_{op}) contribute to crack growth. This is called the effective stress range $\Delta\sigma_{eff}$, which leads to the substitution of ΔK for ΔK_{eff} in (2).

A remarkable feature of PREFFAS is that it does not involve the calculation of a plastic zone size. However, the plastic zone size and therefore the retardation

behaviour is thickness dependent (plane strain / plane stress). The thickness influence in PREFFAS is incorporated via the material constants A and B , which are required for the determination of the crack closure factor U . These constants are thickness dependent. In the following calculations, the actual values for A and B are interpolated from a data base for the material.

A fundamental assumption within PREFFAS is, that the crack growth per GAG cycle is small. Therefore, the spectrum must have a "short recurrence period" [2] and crack growth should not be too close to failure. Otherwise, the crack could have grown out of the dominant plastic zone governing the retardation effect, which would lead to non conservative predictions. Obviously, a short "spectrum" is not a precise definitions, therefore Aliaga [1], one of the developers of the model, has defined a limitation. A crack growth GAG cycle computation with PREFFAS is ruled as valid, as long as the criterion

$$(3) \quad K_{max}/Re < 0.1$$

is fulfilled, where K_{max} is maximum SIF of the spectrum and Re is the yield strength of the material. For the following results, however, the calculations have been performed until critical crack growth, where crack growth is fast. Still, eq. (3) was only violated in the very last GAG-cycles, so that the ignorance of this assumption leads to negligible deviations.

5. RESULTS

In the following the results for both scenarios are discussed. The influence of up to 9 different GAG cycles are analysed.

The damage tolerance analyses have been performed for the, in the damage tolerant design, extensively used aluminium alloy 2024-T3. New materials such as aluminium lithium alloys would be of interest as well. However, Preffas requires additional material parameters A and B , see Sec. 4.2, which are not available in the literature and would need to be determined via coupon testing for multiple thicknesses. A good data basis for AA 2024-T3 is provided in [2]. The used parameters which apply to both scenarios are given in Tab. 2. The detectable half-crack length a_{det} and the scatter

TAB 2. Parameters for both scenarios

Parameter	Value(s)	Unit
rivet diameter	4.0	mm
rivet spacing	20.0	mm
a_{det}	37.5	mm
scatter factor	2.0	-

factor are required for the calculation of the inspection interval. The inspection interval, as used in the following studies, is defined as the number of GAG cycles that are required to grow a crack of size a_{det} to the critical half

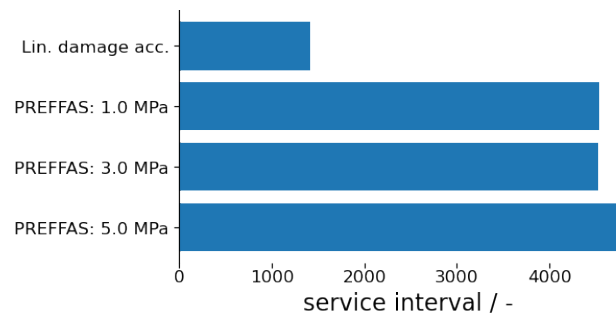


FIG 4. Comparison of service interval for calculations with and with load interaction effects for scenario F with $t_p = 1.5$ mm, $b_s = 200$ mm and $A_s/t_p = 12$ mm, flight 1

crack length, divided by the scatter factor. A different magnitude for these parameters may be used, but this would not change the character of the results. The critical crack size, i.e. the point at which unstable crack growth occurs, is evaluated by means of comparing the SIF at limit load stress with the critical SIF K_c . In other words, unstable crack growth occurs once the residual strength is smaller than the limit load.

Both scenarios feature stiffened structures. The crack is centred under a stiffener which corresponds to a 2-bay-crack. Here, the central stiffener is broken. The 2-bay-crack criterion is fulfilled when the crack tip has reached the next stiffener. The influence of a 2-bay-crack with an intact central stiffener or a 1-bay-crack has been looked into in [7].

5.1. Scenario F: Upper Fuselage

To analyse the extent of the load interaction effects of the GAG cycle, calculations have been performed with the Preffas model and with a simple linear damage accumulation model, which neglects retardation and acceleration effects in Fig 4. In the unfiltered load time histories of the GAG cycles, many small stress-ranges that do not have a significant effect on the fatigue life, as well as noise, are included. By specifying a threshold for the stress range, small stress ranges may be omitted via a racetrack filter, while retaining the original shape of the load sequence. This is obviously crucial for analyses where load interaction effects play a key role. That this is the case here is shown in Fig 4, because the linear damage accumulation underestimates life by 3.2 times. This emphasises the necessity for load interaction models and also shows that considerable interaction effects take place during this kind of load spectrum. PREFFAS computations have been performed for a spectrum where stress ranges below 1 MPa, 3 MPa and 5 MPa have been omitted. For a stress range of 5 MPa the fatigue life time rises, that means that stress ranges have been omitted that were not negligible. Therefore, for this kind of spectrum, an omission range between 1.0 MPa and 3.0 MPa is appropriate.

The calculated inspection intervals due to GAG cycles of flight 1 are shown in Fig 5 for a parameterised

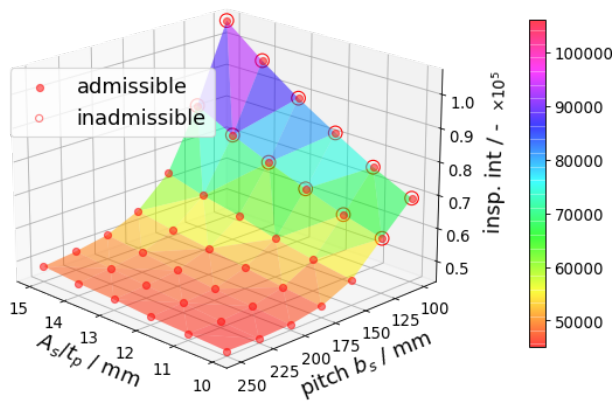


FIG 5. Variation of stringer pitch and stiffening ratio for scenario F with $t_p = 2.5$ mm, flight 1

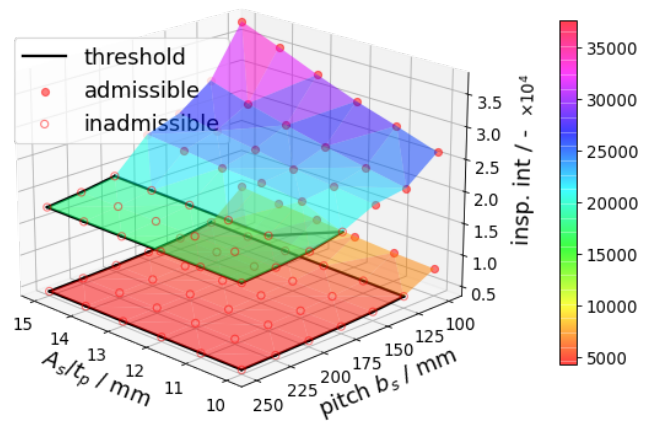


FIG 6. Variation of stringer pitch and stiffening ratio for scenario F with $t_p = 1.5$ mm and $t_p = 2.0$ mm, flight 1

geometry. The parameter space, as could be found in fuselage design, is defined in Tab. 3. The inspection

TAB 3. Parameter intervals Scenario F

Parameter	Interval	Unit
b_s	100.0 - 250.0	mm
t_p	1.5 - 3.5	mm
$A_s/t_p = t_s W_s/t_p$	10.0 - 15.0	mm
fuselage radius	constant	
limit load factor	2.5	-

intervals have been calculated for different stiffener pitches and cross-sections of the stiffeners (red circles). These design variables have a high influence on the aircraft mass and are therefore relevant for preliminary aircraft design. The skin thickness t_p and the fuselage radius are constant. In Fig 5 the 2-bay-crack criterion is fulfilled for all parameter combinations, therefore the results are marked as admissible. For combinations with $b_s \leq 125$ mm, the crack tip has also reached the second stiffener, which is indicated by the second circle enclosing the filled circle. For a skin thickness of $t_p = 2.5$ mm the lowest inspection interval is around 50.000 and increases up to approximately 100.000 for closer spaced stiffeners and stiffeners with a higher cross-section.

Parameter combinations which have not fulfilled the 2-bay-crack criterion are marked as inadmissible, see Fig 6. The inadmissible results are surrounded by the threshold line. The lower and the upper trisurface correspond to a thickness of $t_p = 1.5$ mm and $t_p = 2.0$ mm, respectively. The lower trisurface corresponds to a thickness of $t_p = 1.5$ mm and exhibits low inspection intervals with mostly inadmissible results. A minor increase of 0.5 mm skin thickness leads to a significant rise of the inspection intervals of at least 10.000 GAG cycles.

In the following figures, Fig 5 to Fig 9, the parameterised geometry has been calculated for flights 1-9 for a skin thickness of $t_p = 2.5$ mm. The axis limit for the inspection intervals and the colour bar are fixed, for

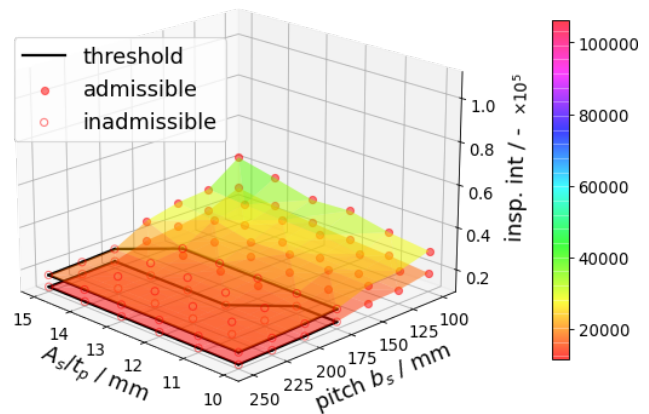


FIG 7. Variation of stringer pitch and stiffening ratio for scenario F with $t_p = 2.5$ mm, surfaces from bottom to top: flight 3, flight 2

better comparability. The figure title gives information about the number of the flight that corresponds to the trisurface.

It should be noted here that the results of the inspection intervals are quite different for the flights. Also the fulfilment of the 2-bay-crack-criterion (admissible/inadmissible) is dissimilar. The results reflect that for flight 3, with the highest stress range (see Tab. 1, integrated spectra), the inspection intervals are indeed the lowest. Although this is not necessarily the case, because of load interaction effects. However, it still is a good indicator for the magnitude of the inspection intervals.

Alike, the flight 4 with a high duration and a high stress range has a low inspection interval as well. In contrast, flight 1 exhibits up to roughly 3 times higher inspection intervals at best.

A very special behaviour occurs for flight 5, which is one of the softer flights. For higher stringer pitches (≥ 125 mm), the inspection intervals are within the ranges of the remaining flights. However for lower stringer pitches the inspection intervals dramatically increases to magnitudes way higher than for other flights. The amounts of circles also reveal, that the crack tip has reached way more stiff-

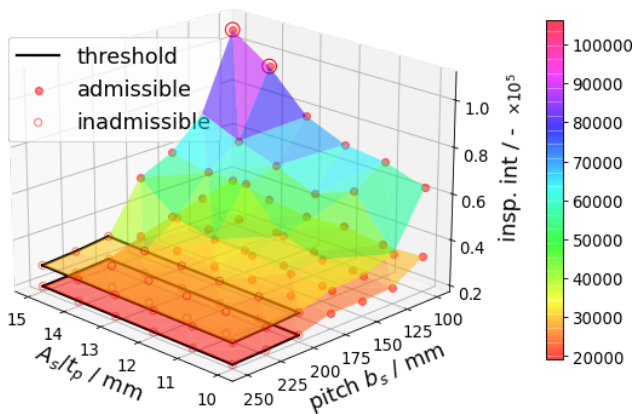


FIG 8. Variation of stringer pitch and stiffening ratio for scenario F with $t_p = 2.5$ mm, surfaces from bottom to top: flight 4, flight 6

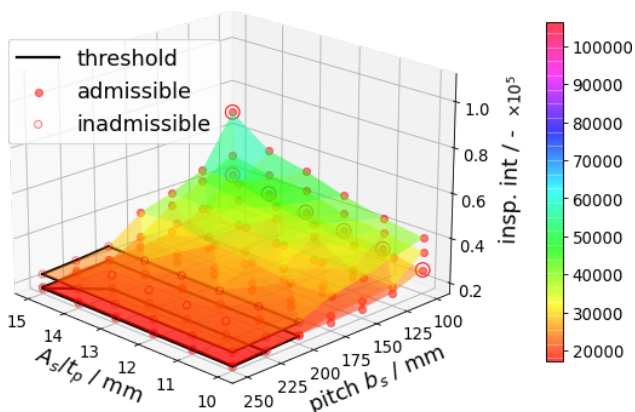


FIG 9. Variation of stringer pitch and stiffening ratio for scenario F with $t_p = 2.5$ mm, surfaces from bottom to top: flight 8, flight 9, flight 7

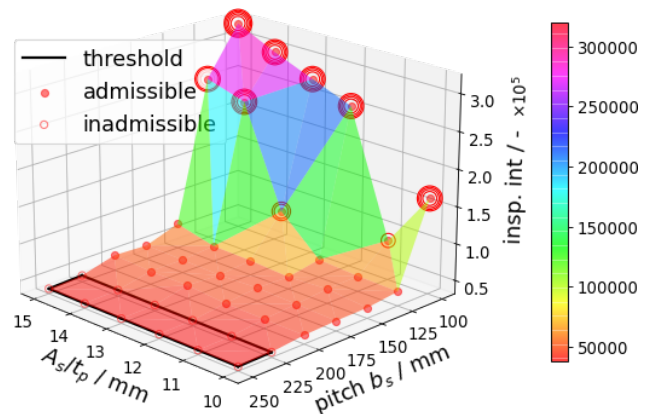


FIG 10. Variation of stringer pitch and stiffening ratio for scenario F with $t_p = 2.5$ mm, flight 5

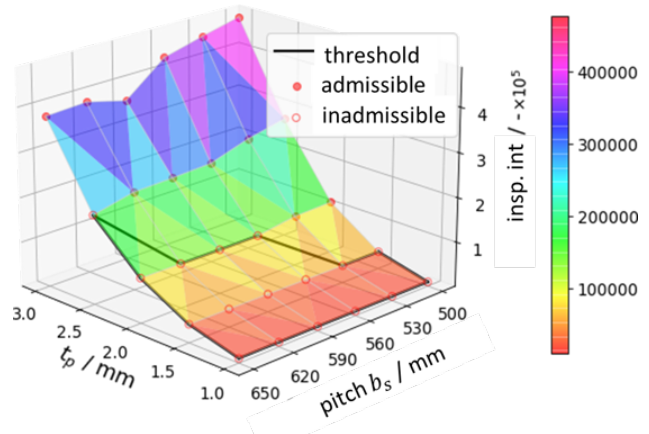


FIG 11. Variation of stringer pitch and panel thickness t_p for scenario F2

eners. In fact, for flight 5, the load is so low, that the crack reaches the next stringer, so that the load is shared between the stringers before a stringer breaks due to exceedance of the yield limit. The sudden decrease of the parameter combinations $A_s/t_p = 11$ mm and $b_s = 100$ mm is assumed to be due to inaccuracies in the SIF determination via the semi-analytical model. It is supposed that an increase in the number of degrees of freedom for the equation system would result in a higher accuracy, removing this outlier, at the cost of computational cost.

5.2. Scenario F2: Fuselage Side

Scenario F2 corresponds to a crack in the longitudinal direction in the fuselage side, which is loaded by the hub stress due to cabin pressurisation. This load cycle is assumed to take place once per flight. Therefore, this is a relative simple scenario with constant amplitude loading and no need for load interaction models. Therefore the following calculation in Fig 11 has been performed via the linear damage accumulation. In a pressurised fuselage, the internal pressure acting on crack edges results in out-of-plane deformation, so-called bulging. This results in higher SIFs, which is considered via an additional correction factor β in (1). The inspection intervals for Fig 11 are already very high for a low skin thickness

of $t_p = 1.0$ mm. However, these results are inadmissible because the crack tips do not reach the first frame. Therefore the fulfilment of the 2-bay-crack criterion is the structural problem and not the magnitude of the inspection interval.

6. CONCLUSION

Two realistic scenarios for a passenger aircraft are investigated, featuring the upper fuselage panel (scenario F) and a fuselage side panel (scenario F2). These scenarios are relevant for aircraft design and results from a damage tolerance design point of view are presented.

The damage tolerance analyses are performed via cycle-by-cycle crack-growth computations with load interaction effects modelled via the crack closure model PREFFAS. A quick overview about the limitations of the PREFFAS model is given in [9]. A model which considers the delayed retardation effect would increase the physical soundness of the model and the quality of the results. The impact of negative stresses is ignored by Preffas. While the crack is closed during a negative stress, and thus no crack growth occurs following (2), the negative stresses do have a systematic effect on the crack closure because these affect the residual stresses

in the plastic wake which govern the crack closure. This is of importance for ground loads, such as the landing impact.

The inspection intervals for the different flights (with fixed geometry) vary up to a factor of 3. The significance of the strength of the stiffeners has been shown for flight 5, where the soft flight is able to extend the fatigue life time dramatically, because the stiffeners have not failed.

7. ACKNOWLEDGEMENT

The authors thankfully acknowledge the funding of the work presented here in the IMeLa project within the German Luftfahrtforschungsprogramm under project number 20A1709D.

Contact address:

fa.runge@tu-braunschweig.de

References

- [9] S Khan, René Alderliesten, Jaap Schijve, and R. Benedictus. On the fatigue crack growth prediction under variable amplitude loading.
- [1] D Aliaga, A Davy, and H Schaff. A simple crack closure model for predicting fatigue crack growth under flight simulation loading. In Jc Newman and W Elber, editors, *Mechanics of Fatigue Crack Closure*, pages 491–491–14. ASTM International. DOI: [10.1520/STP27227S](https://doi.org/10.1520/STP27227S).
- [2] J. Schijve. An evaluation of a fatigue crack growth prediction model for variable-amplitude loading (PREFFAS). Publisher: Delft University of Technology.
- [3] Emy Arts. A novel approach to flight phase identification using machine learning.
- [4] John W. Rustenburg, Donald Skinn, and Daniel O. Tipps. Development of an improved maneuver-gust separation criterion.
- [5] John W. Rustenburg, Donald Skinn, and Daniel O. Tipps. An evaluation of methods to separate maneuver and gust load factors from measured acceleration time histories. Section: Technical Reports.
- [6] Fazle Karim, Somshubra Majumdar, Houshang Darabi, and Shun Chen. LSTM fully convolutional networks for time series classification. DOI: [10.48550/ARXIV.1709.05206](https://doi.org/10.48550/ARXIV.1709.05206).
- [7] Michael Rohdenburg, Fabian Runge, Matthias Haupt, Lennart Markgraf, Peter Horst, and Sebastian Heimbs. HOLISTIC LOW-EFFORT MODEL FOR DAMAGE TOLERANCE ANALYSIS IN PRELIMINARY DESIGN. 2022(3):1–20. DOI: [10.2478/tar-2022-0013](https://doi.org/10.2478/tar-2022-0013).
- [8] Toshihiko Nishimura. Stress intensity factors for a cracked stiffened sheet with cracked stiffeners. 113(1):119–124. DOI: [10.1115/1.2903366](https://doi.org/10.1115/1.2903366).